Asian Power Electronics Journal, Vol. 12, No. 2, June 2018

Comparison Study of Rare-earth-free Motors with Permanent Magnet Motors in EV Applications

Zhu J. W. Cheng K. W. E. Xue X. D.

Abstract-Four topologies of in-wheel motors, including three switched reluctance motors and one permanent magnet synchronous motor of the same dimension, are proposed for comparison in electric vehicle applications. The three switched reluctance motors are 6/4, 6/10 and 6/16 two-teeth structures, respectively, along with the permanent magnet synchronous motor topology of 12 stator slot and 8 poles. The parameters of the motors are optimized for the best torque performance through genetic algorithm. The comparison contains torque output, iron loss and efficiency. Consequently, the results demonstrate 6/16 two-teeth switched reluctance topology is a potential candidate for electric vehicle applications.

Keywords-Finite element analysis, torque, iron loss, efficiency

I. INTRODUCTION

Owing to its efficient utilization of energy and ability to relieve environmental pollution in urban areas, the electric vehicle (EV) is receiving more and more attention. As a major power supply for vehicle operation, electric machines own the dominant advantage of much higher efficiency compared with the internal combustion engine (ICE), which may own even less than 20% efficiency for vehicle application. Therefore, the design of electric machines for EV application is quite a hot topic nowadays.

Electric machines can be divided into two categories: permanent magnet (PM) machines and rare-earth free machines. The PM motor owns a dominant position in EV applications due to its features of higher torque density and lower volume. It can also be classified into two groups on the basis of PM position: permanent magnet sychronous motor (PMSM) with PM on the rotor and flux switching motor (FSM) with PM inserted into the stator. Both of them have been applied widespread to EVs.

A thermal model of a water-cooled PMSM for EV propulsion is proposed to avoid demagnetization of PM material [1]. Design strategies of variable flux permanent magnet synchronous machine (VF-PMSM) are put forward to meet the requirement of reduced loss [2]. A vector flux-weakening control method is developed to extend motor speed range for EV drive system [3]. A new sound quality evaluation method of noise of PMSM is proposed in [4]. A novel calculation method on current charateristics of a vector inverter is proposed [5].

A Partitioned-Stator FSM with mechanical parts is proposed for EVs [6]. A high torque density and efficiency FSM with robust rotor structure is analyzed for high power applications [7]. A novel FSM with PM inserted in the rotor is developed in [8]. Kim [9] proposes a novel axial FSM to eliminate even harmonics for EV applications.

For the application of rare-earth free motors to EVs, the switched reluctance motor (SRM) occupies the major part due to its features of simple and robust configuration, fault tolerant capability and wide speed range. Design and analysis of a high-torque-density rotor segmented SRM is proposed for direct drive application [10-11]. A high efficiency and torque density SRM is developed for vehicle propulsion [12]. Chiba proposes a high torque density of 45Nm/L SRM for hybrid vehicles [13].

For EV applications, FSM is not as competitive as PMSM for in-wheel applications as a result of high magnetic saturation in the stator caused by coexistence of armature windings and PM material [7], limited area for copper windings [14]. Therefore, in this paper, PMSM and SRM are selected as comparison candidates. The SRMs contain a conventional 6/4 SRM, a 6/10 SRM with more rotor poles than stator poles [15] and a 6/16 SRM combining more rotor poles than stator teeth and multiple teeth per stator pole together [16], while the PMSM is a surface-mounted type. All of the four topologies are in-wheel version for comparison. Section II illustrates the characteristics of the motor topologies and their design considerations. Section III put forward the performance comparison of the four motors, including torque output, iron loss and efficiency. Section IV concludes the whole paper.

II. CHARACTERISTICS ANALYSIS & DESIGN CONSIDERATIONS FOR THE FOUR MOTORS

From theoretical analysis, the torque formula of the PMSM can be expressed as follows:

$$T_e = \frac{3}{2} p[\frac{(L_q - L_d)}{2} I_m^2 \sin 2\varphi_i + I_m \psi_m \cos\varphi_i] \quad (1)$$

where p is the pole pair number, I_m is the peak value of sinusoidal current, ψ_m is the PM excited flux linkage, φ_i is the internal power factor angle, L_q and L_d is the inductance of q axis and d axis, respectively. For surface-mounted PMSM, L_q is equal to L_d, so the torque equation can be simplified as,

$$T_e = \frac{3}{2} p I_m \psi_m \cos\varphi_i \quad (2)$$

For the SRM, the torque formula can be obtained from,

Power Electronics Research Center, Department of Electrical Engineering, The Hong Kong Polytechnic University, Hong Kong
E-mail: jingwei.zhu@connect.polyu.hk

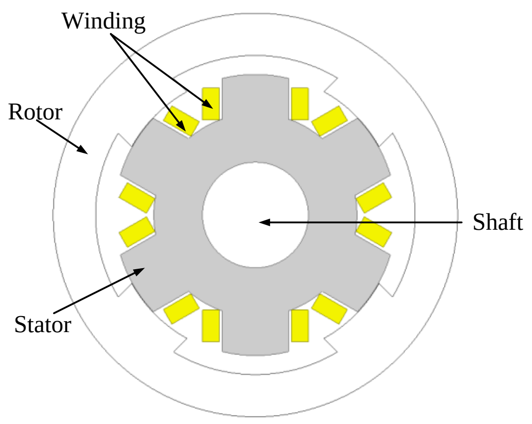

Fig. 1: (a) 6/4 SRM

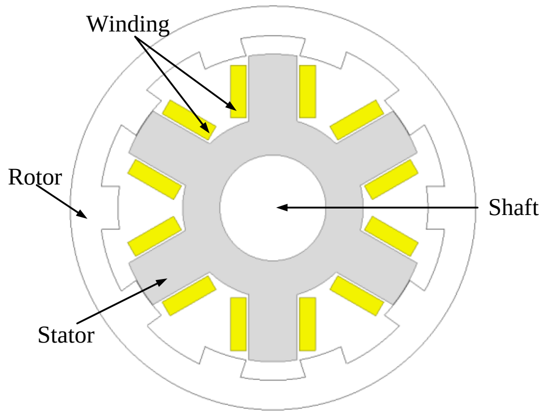

Fig. 1: (b) 6/10 SRM

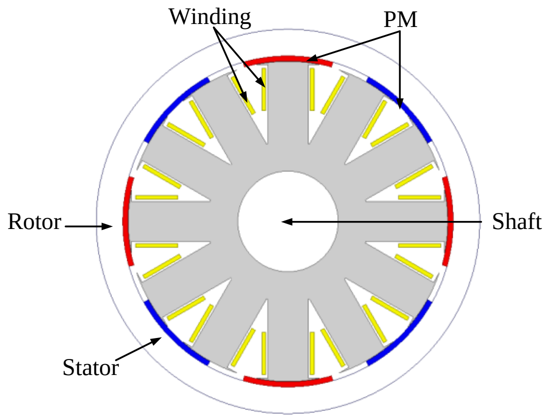

Fig. 1: (c) 12-stator-slot 8-pole PMSM

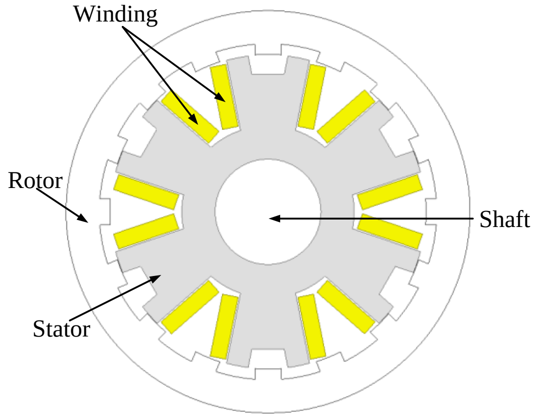

Fig. 1: (d) 6/16 two-teeth SRM

$$T_e = \frac{\partial W_m}{\partial \theta} \tag{3}$$

where W_m is the field co-energy and θ is the rotor position. The torque can be calculated further as [16],

$$T_e = \int \frac{N^2 I \mu_0 m l r}{2 l_g} di \tag{4}$$

where m is the number of teeth per pole, r is the outer radius of the stator, l_g and l is the airgap and stack length, respectively; μ_0 is magnetic permeability in the vacuum and N is number of turns per phase.

For in-wheel applications, the overall dimension of the motors should be determined initially. Because of the inner stator and outer rotor structure, the outer rotor diameter is selected as 382 mm, same as that in [17]. Due to the limitation of the wheel width, the stack length is set as 74 mm and the airgap length is chosen as 0.5 mm. The SRMs are 6/4, 6/10 and 6/16 topology, separately, while the PMSM is 12 stator slot and 8 PM poles.

For the optimization process, genetic algorithm (GA) method is utilized for multi-variable optimization. The objective function is the torque output. As a consequence of air cooling condition for in-wheel applications, the current density is limited to 5A/mm^2. Because of concentrated winding topology, the slot packing factor is selected as 0.44. By setting a suitable population number, maximum generation, crossover probability, elite count and mutation ratio, and utilizing rank fitness scaling, stochastic uniform selection, the final optimized four motor topologies are shown in Fig. 1. Besides, their parameters can be obtained from Table I.

Table I
Basic Parameters of the Four Motors

Dimensions	6/4 SRM	6/10 SRM	12/8 PMSM	6/16 SRM
Rotor outer diameter D_{r2} (mm)	382	382	382	382
Stator outer diameter D_{s2} (mm)	274	291	318	298
Stack length l (mm)	74	74	74	74
Airgap length l_g (mm)	0.5	0.5	0.5	0.5
Stator pole/teeth arc angle θ_s (degree)	27	18	22.5	8
Rotor pole arc angle θ_r (degree)	32	16	-	9.5
Number of turns per phase N	132	248	192	204
PM thickness (mm)	-	-	5	-
PM arc angle (degree)	-	-	31.5	-
Steel type	DR510	DR510	DR510	DR510
Copper wire diameter (mm)	1.12	1.12	1.12	1.12
Number of parallel windings	8	8	8	8
Slot fill factor	0.44	0.44	0.44	0.44

III. Performance Analysis & Comparison

The performance of the four topologies is calculated and analyzed by using finite element method (FEM), including torque characteristics, energy loss, power output and efficiency.

A. Comparison of three SRMs

For conventional SRMs, the torque density is relatively lower due to the elimination of PM materials. The 6/10 SRM is able to enlarge the slot area for more copper windings by increasing the number of rotor poles in order to provide enough torque output. The 6/16 two-teeth topology owns the capability to enhance torque output by enabling magnetic flux to pass through two divided teeth and enlarging the area for windings as illustrated in equation (4). The curves of the flux linkage of the three SRMs based on FEM at the unaligned and aligned position can be acquired from Fig. 2. Besides, the torque curve of one-phase conducting with the rated current during half an electric period can be obtained from Fig. 3 with the unaligned position set as zero degree.

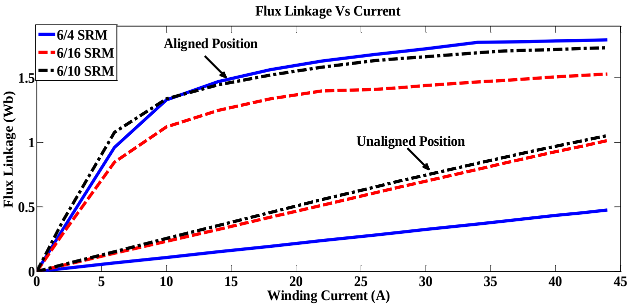

Fig. 2: Flux linkage of the three SRMs

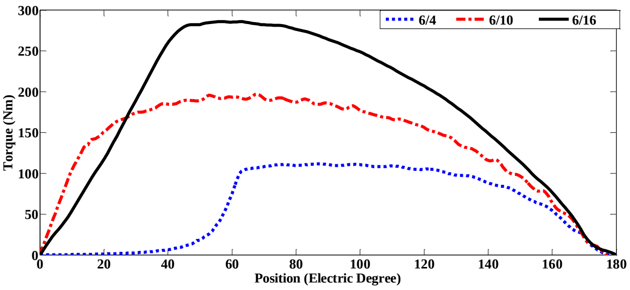

Fig. 3: Torque curves of SRMs for half an electric period conducting

Although the difference between the aligned and unaligned position for 6/10 and 6/16 SRM topologies is smaller than that of 6/4 SRM, the number of striking times for 6/10 SRM is 2.5 times as many as that for 6/4 SRM and the multiple teeth topology of 6/16 SRM doubles the striking times, along with increasing the striking times by more rotor poles. The torque improvement of 6/10 and 6/16 SRMs is demonstrated in Fig. 3 indicating the advancement of the topologies.

B. Comparison of PMSM with SRMs

The comparison is on the basis of in-wheel motors for EV applications. The current density is limited to 5A/mm^2 because of air cooling condition and the rated speed is 1000 rpm. The magnetic flux densities of the four motors at rated power are shown as below in Fig. 4.

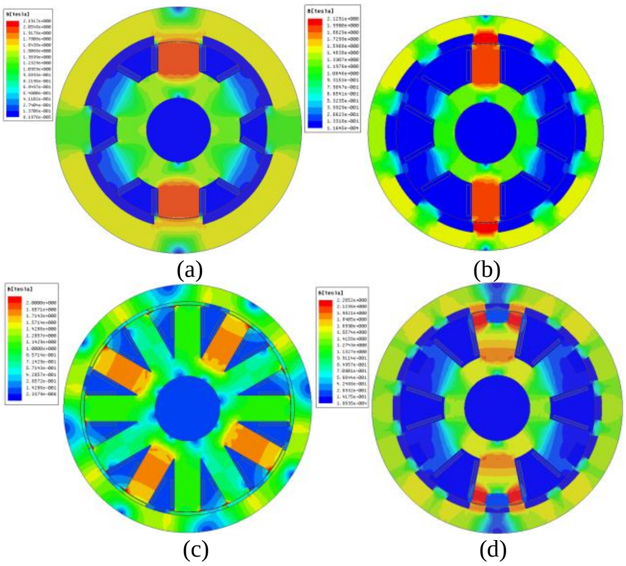

Fig. 4: Magnetic flux density of (a) 6/4 SRM (b) 6/10 SRM (c) 12/8 PMSM (d) 6/16 two-teeth SRM

The torque performance of the above four topologies at the rated speed with full phase conducting can be obtained from Fig. 5 by using FEM.

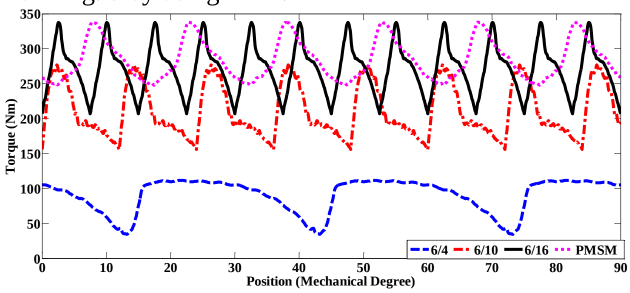

Fig. 5: Torque characteristics comparison of the four topologies

Fig. 5 illustrates that 6/16 two teeth SRM is able to provide comparable torque output with the PMSM. The high torque feature of this rare-earth free SRM demonstrates its potential for EV applications. Moreover, the total iron loss and motor theoretical calculated efficiency by utilizing FEM is shown in the following Fig. 6 and Fig. 7 under various speed condition.

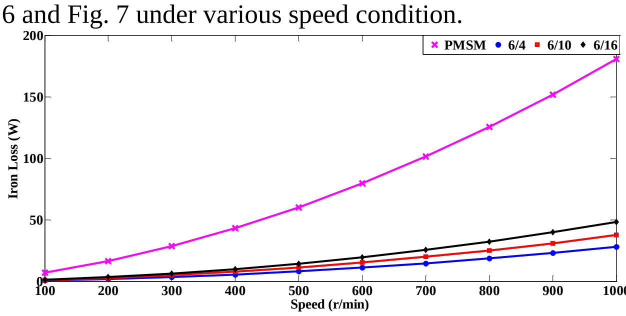

Fig. 6: Iron loss comparison under different speeds

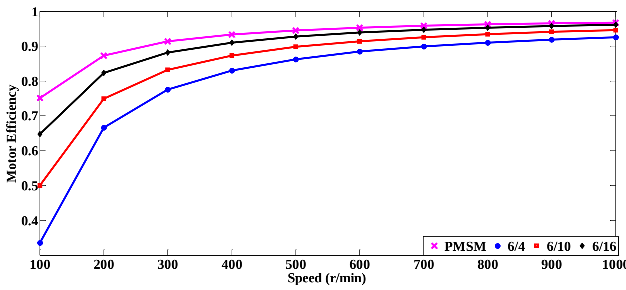

Fig. 7: Calculated motor efficiency comparison under various speeds condition

The comparison results in Fig. 6 show that the total iron loss of the PMSM is much higher than three SRMs due to the fact that the PMSM owns both core loss from the steel and eddy current loss from the PM material. 6/10 and 6/16 two-teeth SRM topology also increase total iron loss compared with the conventional counterpart because of smaller commutation angle and higher frequency of commutation. However, the iron loss of them is not as significant as that of the PMSM.

The efficiency comparison results shown in Fig. 7 demonstrate that the PMSM exhibits the highest efficiency for in-wheel applications. The existence of considerable copper loss due to more copper windings for SRMs decreases their efficiencies. The PMSM increases iron loss by utilizing PM material, but weakens its own copper loss more, thus leading to higher efficiency compared with other kinds of machines. 6/16 two-teeth SRM, however, also exhibits high efficiency for EV applications, which is quite similar to that of the PMSM at the rated speed. Additionally, 6/16 SRM topology does not contain any rare-earth materials. Therefore, it can be selected as an ideal candidate for the EV in-wheel motor. The performance comparison of the four topologies at the rated speed 1000 r/min can be found in the following Table II.

Table II
Performance Comparison of the Four Topologies

Dimensions	6/4 SRM	6/10 SRM	12/8 PMSM	6/16 SRM
Current density (A/mm^2)	5	5	5	5
RMS current (A)	39.4	39.4	39.4	39.4
Iron loss (W)	28	38	181	48
Copper loss (W)	576	1006	670	916
Torque (Nm)	91	209	284	271
Torque ripple (%)	85	58	32	48
Rated power (kW)	9.5	22	30	28
Coil end length (mm)	16	18	11	15
Torque density (Nm/L)	7.5	16.1	25.8	22.8
Efficiency (%)	92.6	94.6	96.7	96.2

From the above Table II, the torque density and efficiency of 6/16 SRM are quite similar to those of a PMSM. As a result, it can be considered as a competitive candidate for a high torque density rare-earth free in-wheel motor.

IV. Conclusion

In this paper, four topologies of in-wheel electric machines, including a surface-mounted PMSM and three SRMs, namely 6/4, 6/10 and 6/16 structures, are proposed for performance comparison. All the topologies are optimized for maximal torque output. The following analysis based on FEM demonstrates that 6/16 two-teeth SRM is able to provide comparable torque density with the PMSM of the same dimension, while conventional and 6/10 SRM exhibits much lower performance. Besides, the efficiency of it is quite similar to that of a PMSM. Therefore, it owns a vast potential for EV applications due to its rare-earth free feature.

Reference

[1] Bin Zhang, Ronghai Qu, Jin Wang, Wei Xu, Xinggang Fan, and Yu Chen, "Thermal Model of Totally Enclosed Water-Cooled Permanent-Magnet Synchronous Machines for Electric Vehicle Application", *IEEE Trans. Ind. Appl.*, vol. 51, no. 4, pp. 3020–3029, Jul./Aug. 2015.

[2] Apoorva Athavale, Kensuke Sasaki, Brent S. Gagas, Takashi Kato, and Robert D. Lorenz, "Variable Flux Permanent Magnet Synchronous Machine (VF-PMSM) Design Methodologies to Meet Electric Vehicle Traction Requirements with Reduced Losses", *IEEE Trans. Ind. Appl.*, vol. 53, no. 5, pp. 4318–4326, Sep./Oct. 2017.

[3] Yue Zhang, Wenping Cao, Sean McLoone, and John Morrow, "Design and Flux-Weakening Control of an Interior Permanent Magnet Synchronous Motor for Electric Vehicles", *IEEE Trans. Appl. Supercond.*, vol. 26, no. 7, Oct. 2016.

[4] Conggan Ma, Qing Li, Qinghe Liu, Dafang Wang, Jiajun Gao, Huiyao Tang, and Yanhua Sun, "Sound Quality Evaluation of Noise of Hub Permanent-Magnet Synchronous Motors for Electric Vehicles", *IEEE Trans. Ind. Electron.*, vol. 63, no. 9, pp. 5663–5673, Sep. 2016.

[5] Ki-Chan Kim, "A Novel Calculation Method on the Current Information of Vector Inverter for Interior Permanent Magnet Synchronous Motor for Electric Vehicle", *IEEE Trans. Magn.*, vol. 50, no. 2, Feb. 2014.

[6] Christopher H. T. Lee, James L. Kirtley, Jr., and M. Angle, "A Partitioned-Stator Flux-Switching Permanent-Magnet Machine With Mechanical Flux Adjusters for Hybrid Electric Vehicles", *IEEE Trans. Magn.*, vol. 53, no. 11, Nov. 2017.

[7] Wei Hua, Gan Zhang, and Ming Cheng, "Investigation and Design of a High-Power Flux-Switching Permanent Magnet Machine for Hybrid Electric Vehicles", *IEEE Trans. Magn.*, vol. 51, no. 3, Mar. 2015.

[8] Peng Su, Wei Hua, Gan Zhang, Zhe Chen, Ming Cheng, "Analysis and evaluation of novel rotor permanent magnet flux-switching machine for EV and HEV applications", *IET Electr. Power Appl*, vol. 11, no. 9, pp. 1610-1618, 2017.

[9] Ju Hyung Kim, Yingjie Li, and Bulent Sarlioglu, "Novel Six-Slot Four-Pole Axial Flux-Switching Permanent Magnet Machine for Electric Vehicle", *IEEE Trans. Transport. Electrific.*, vol. 3, no. 1, pp. 108–117, Mar. 2017.

[10] Saurabh P. Nikam, Vandana Rallabandi, and B. G. Fernandes, "A High-Torque-Density Permanent-Magnet Free Motor for in-Wheel Electric Vehicle Application", *IEEE Trans. Ind. Appl.*, vol. 48, no. 6, pp. 2287–2295, Nov./Dec. 2012.

[11] Vandana Rallabandi, Baylon Godfrey Fernandes, "Design procedure of segmented rotor switched reluctance motor for direct drive applications", *IET Electr. Power Appl*, vol. 8, no. 3, pp. 77-88, 2014.

[12] Khwaja M. Rahman and Steven E. Schulz, "Design of High-Efficiency and High-Torque-Density Switched Reluctance Motor for Vehicle Propulsion", *IEEE Trans. Ind. Appl.*, vol. 38, no. 6, pp. 1500–1507, Nov./Dec. 2002.

[13] Akira Chiba, Kyohei Kiyota, Nobukazu Hoshi, Masatsugu Takemoto, and Satoshi Ogasawara, "Development of a Rare-Earth-Free SR Motor With High Torque Density for Hybrid Vehicles", *IEEE Trans. Energy Convers.*, vol. 30, no. 1, pp. 175–182, Mar. 2015.

[14] Z. Q. Zhu and J. T. Chen, "Advanced Flux-Switching Permanent Magnet Brushless Machines", *IEEE Trans. Magn.*, vol. 46, no. 6, pp. 1447-1453, Jun. 2010.

[15] Berker Bilgin, Ali Emadi and Mahesh Krishnamurthy, "Design Considerations for Switched Reluctance Machines With a Higher Number of Rotor Poles", *IEEE Trans. Ind. Electron.*, vol. 59, no. 10, pp. 3745–3756, Oct. 2012.

[16] Jingwei Zhu, Ka Wai Eric Cheng, Xiangdang Xue, Yu Zou, "Design of a New Enhanced Torque In-Wheel Switched Reluctance Motor with Divided Teeth for Electric Vehicles", *IEEE Trans. Magn.*, vol. 53, no. 11, Nov. 2017.

[17] X. D. Xue, K.W.E. Cheng, T.W. Ng, and N. C. Cheung, "Multi-Objective Optimization Design of In-Wheel Switched Reluctance Motors in Electric Vehicles", *IEEE Trans. Ind. Electron.*, Vol. 57, No. 9, pp. 2980 – 2987, Sep. 2010.